Available online at www.sciencedirect.com
ScienceDirect
Trans. Nonferrous Met. Soc. China 24(2014) 431−440
Transactions of Nonferrous Metals Society of China
www.tnmsc.cn

Properties improvement and microstructure changes during thermomechanical treatment in sintered Cu−Au alloy

Ivana MARKOVIC, Svetlana NESTOROVIC, Desimir MARKOVIC, Dragoslav GUSKOVIC

Technical Faculty in Bor, University of Belgrade, VJ 12, 19210 Bor, Serbia

Received 13 June 2013; accepted 12 September 2013

Abstract: The changes in hardness, microhardness, electrical conductivity and microstructure of the sintered Cu−4%Au (mole fraction) alloy during thermomechanical treatment were studied. Following the primary strain hardening, an annealing of rolled alloy in the temperature range of 60−350 °C provided additional strengthening due to the anneal hardening effect. An increase in properties took place in two stages, and the best combination of properties was achieved in the alloy pre-rolled with 40% reduction after annealing at 260 °C. Significant microstructural changes followed the changes of properties in the course of the thermomechanical treatment.

Key words: Cu−Au alloys; anneal hardening; thermomechanical treatment; hardness; microhardness; electrical conductivity

1 Introduction

Continuous technological progress demands the production of strengthened alloys having not only high mechanical properties, but also high electrical conductivity and good corrosion resistance [1]. Copper-based alloys display an attractive combination of properties: excellent electrical and thermal conductivity, relatively good mechanical properties and resistance to softening at high temperatures, high corrosion resistance and good formability [2]. Among the copper-based alloys, Cu−Au alloys have a wide range of applications for coating, high temperature devices, catalysis, electronic industry, jewelry and dental applications [3,4]. The Cu−Au system has been the subject of numerous studies as a typical system with order−disorder phase transformations that contribute to an increase in mechanical properties and a reduction in ductility. According to the Cu−Au phase diagram, the Cu−4Au alloy chosen for this study is a disordered or short-range ordered solid solution, and long-range ordering does not occur in it [5]. When this alloy is heated to a higher temperature, copper and gold atoms take random positions, making a disordered solid solution. Quenching at this stage prevents any possible formation of a long-range ordered arrangement of copper and gold atoms. During the low temperature annealing of such disordered solid solution after cold deformation, a significant strengthening occurs. The described phenomenon is known as the anneal hardening effect [6,7]. It has been mainly studied in some copper-based alloys, especially in Cu−Al and Cu−Zn binary systems. The origin of anneal hardening has not been fully determined. Some studies have interpreted it as a result of atomic ordering due to interactions between different atoms [8−10]. However, in some other experiments, it was concluded that solute segregation to dislocations and the locking of the dislocations had the greatest impact, although solute segregation to other stacking faults could not be ignored [6,7,11−13].

One of the most systematic studies about the influence of the alloying elements on the intensity of the anneal hardening effect was studied by VITEK and WARLIMONT [6]. The mentioned study confirmed the largest increase in spring bending limit σ_{bE} (measure of anneal hardening effect) in the Cu−Au system, among seven copper binary systems with Al, Zn, Ga, Ni, Au, Pd and Rh. However, no work has been found on the anneal hardening effect in sintered copper alloys (except a few written by the author of this work [14−16]), and the studies of anneal hardening in the cast Cu−Au alloys

Foundation item: Project (TR34003) supported by the Ministry of Education, Science and Technological Development of the Republic of Serbia
Corresponding author: Ivana MARKOVIC; Tel: +381-30-424555; Fax: +381-30-421078; E-mail: imarkovic@tf.bor.ac.rs
DOI: 10.1016/S1003-6326(14)63079-X

have also been limited [6]. For these two reasons, the anneal hardening effect in sintered Cu−Au alloy was studied.

2 Experimental

Electrolytic copper powder (purity of 99.97%) and gold powder (purity of 99.93%) were used as starting materials in this experiment. Obtaining of the sintered samples was performed according to the common powder metallurgy procedure which included mixing of powders, compacting of the mixture and sintering of compacts. A copper-based powder mixture containing 4% (mole fraction) of gold powder was mixed without any binder in the tri-axial Turbula mixer for 2 h. The homogenized mixture was compacted into prism-shaped green compacts with dimensions of 12 mm in width, 30 mm in length and 6−6.5 mm in height, using a pressure of 360 MPa in a Mohr-Federhaff-Losenhausen hydraulic press. The green compacts were then sintered in the T-40/600 tube furnace at 850 °C for 1 h under hydrogen atmosphere. The thermomechanical treatment applied to the sintered samples of Cu−4Au alloy consisted of pre-final rolling, heat treatment with quenching, final rolling and isochronal annealing. Pre-final cold-rolling to the calculated heights of 5, 3.3, 2.5 and 2 mm (with 20.4%, 44.5%, 57.6% and 66.7% reductions, respectively) was carried out at room temperature on a Marshall Richard rolling mill. The rolling reduction (ε) is defined as $\varepsilon=((H_o-H)/H_o)\times100\%$, where H_o is the initial sample height and H is the sample height after rolling. Pre-finally rolled samples were then subjected to the heat treatment at 500 °C for 45 min under hydrogen atmosphere, followed by cold water quenching. After that, the final cold-rolling with 60%, 40% and 20% reductions on the final height of 2 mm was performed. Quenched and finally rolled samples with 20% and 40% reductions were subsequently isochronally annealed for 30 min at temperatures between 60 °C and 700 °C.

The changes in hardness, microhardness, electrical conductivity and microstructure were measured during the complex thermomechanical treatment which was used to create the conditions for the occurrence of the anneal hardening effect. Hardness values were measured using the VEB Leipzig Vickers hardness tester with a load of 49 N and a dwell time of 15 s. Microhardness measurements were performed on a PMT-3 Vickers microhardness tester with a load of 0.98 N and a dwell time of 15 s. Electrical conductivity values were determined using the Sigmatest instrument. At least eight measurements of hardness, microhardness and electrical conductivity were performed on each sample. The results were averaged and reported as a single data point with its variation interval. All measurements were carried out on the rolling plane. Microstructures of the Cu−4Au alloy samples, in the various stages of thermomechanical treatment, were examined using a Carl Zeiss Jena optical microscope (OM) and Jeol JSM-6610LV scanning electron microscope (SEM) with an EDS detector. For the microstructural examination, samples were ground, polished using 0.05 μm alumina powders and etched with an aqueous solution containing 10% KCN and 10% $(NH_4)_2S_2O_8$ in a one to one ratio.

3 Results and discussion

3.1 Influence of pre-final and final rolling on properties and microstructure

Figure 1 shows the SEM micrographs, and Fig. 2 shows the OM images of the sintered Cu−4Au alloy before and after the pre-final and final cold-rolling. The metallographic surfaces of the pre-finally and finally rolled samples were both parallel (longitudinal plane) and perpendicular (transverse plane) to the rolling direction.

The microstructure of the alloy after sintering at 800 °C for 1 h (Figs. 1(a) and 2(a)) consists of equi-axed grains of the alpha phase (solid solution of gold in copper). A fine-grained structure with a grain size in the range of 5−20 μm can be seen. Spherical pores are visible within the grains and especially along the grain boundaries.

Figures 1(b) and 2(b) show the microstructure of the sintered alloy after the pre-final rolling with 44.5% reduction. In the process of plastic deformation, crystal lattice rotates and tends to place itself in the advantageous position in the direction of deformation [17]. Therefore, the equi-axed grains are deformed and elongated in the rolling direction, and flattened in a direction perpendicular to the rolling direction. Also, it is noted that the pores are no longer spherical, but stretched in the rolling direction.

The microstructure of the alloy sample quenched from 500 °C is shown in Figs. 1(c) and 2(c). After the pre-final rolling, samples were quenched to conserve the structure existing at higher temperatures. Solute atoms of gold are trapped in disadvantageous positions, creating a disordered solid solution. During the heat treatment, recrystallization occurs with the growth of new and un-deformed grains. Therefore, the microstructure of the quenched sample consists of polygonal grains with noticeably straight and flat grain boundaries. A large number of annealing twins appear in the microstructure due to the creation of double lines or bands as a result of shearing. These pores are homogeneously distributed, are spherical again and also smaller than those in the sintered condition.

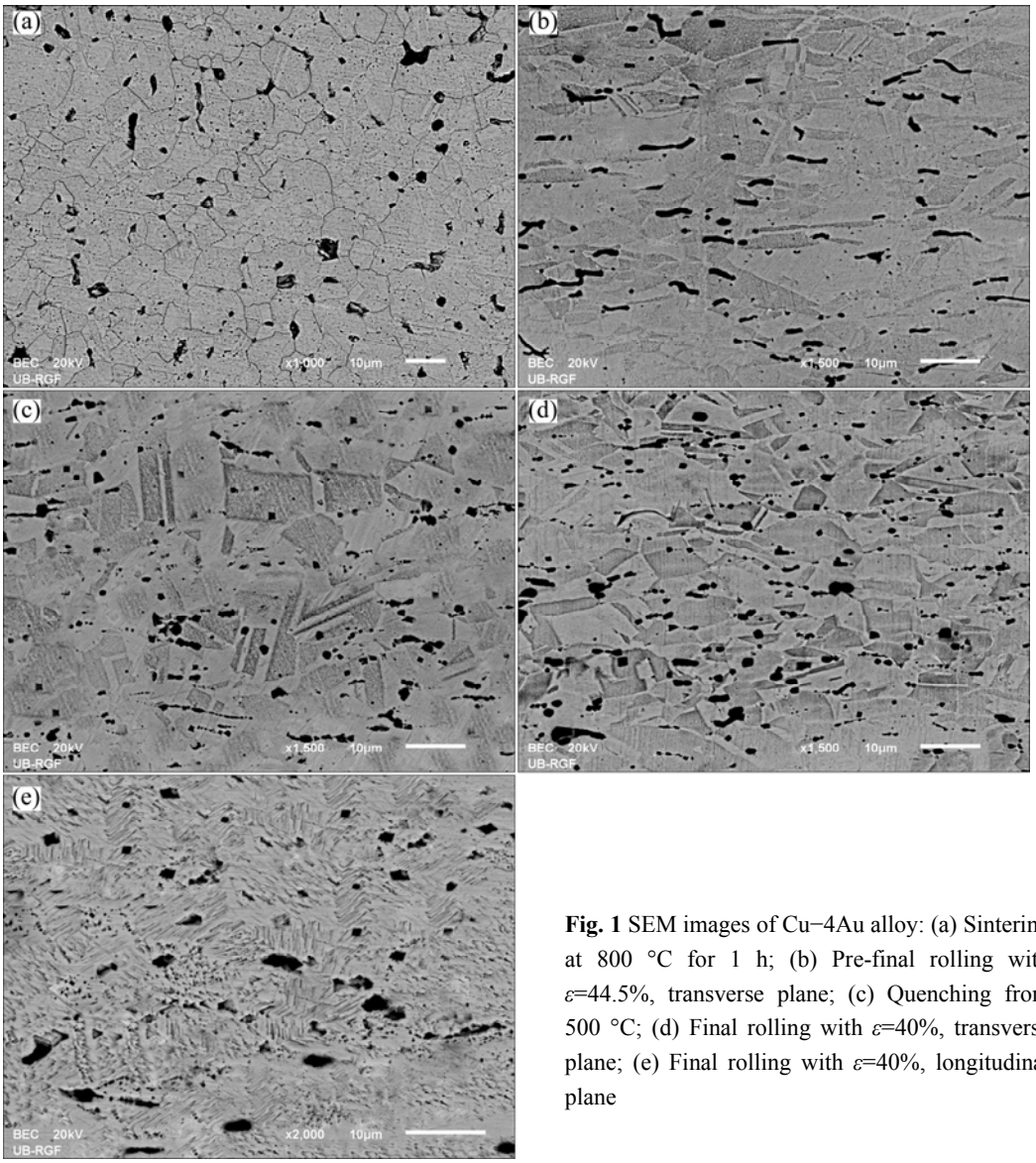

Fig. 1 SEM images of Cu−4Au alloy: (a) Sintering at 800 °C for 1 h; (b) Pre-final rolling with ε=44.5%, transverse plane; (c) Quenching from 500 °C; (d) Final rolling with ε=40%, transverse plane; (e) Final rolling with ε=40%, longitudinal plane

The subsequent plastic deformation of the quenched samples by final rolling with 40% reduction causes a significant change in their microstructure, as shown in Figs. 1(d), 1(e), 2(d) and 2(e). The cross-sectioned grains are flattened and have noticeably defined grain boundaries. The longitudinally sectioned grains are elongated and aligned in the same direction, but do not have clearly defined boundaries. During the rolling, the dislocations move along the slip planes, causing the steps as a result of intersection of the slip planes and the crystal surface [18]. These steps, named slip lines or slip traces, exhibit in the microstructure, as shown in Figs. 1(e) and 2(e). Long and straight slip lines are noticeable in some grains, and their existence demonstrates that plastic flow is not uniform [19].

The described microstructural changes caused by the change in the state of thermomechanical treatment were reflected in the improvement of properties of Cu−4Au alloy. Figure 3 shows the influence of rolling reduction on the hardness values during the pre-final and final cold-rolling. The pre-final rolling was carried out on the sintered samples while the final rolling was carried out on the quenched samples. The hardness of all samples was improved during both cold-rollings due to the generation of dislocations. Dislocations interact with gold solute atoms and with other generated dislocations, which become increasingly immovable during the cold-rolling, causing the deformation strengthening of the alloy. The further increase in mechanical properties with increasing rolling reduction is more pronounced because of the increase in lattice imperfections [20]. The initial microstructure (sintered or quenched) has an important effect on the deformation behaviour of the alloy. The hardness value of the sintered sample is HV63 and it increases to HV140 after the pre-final rolling with 66.7% reduction. In the quenched condition, the

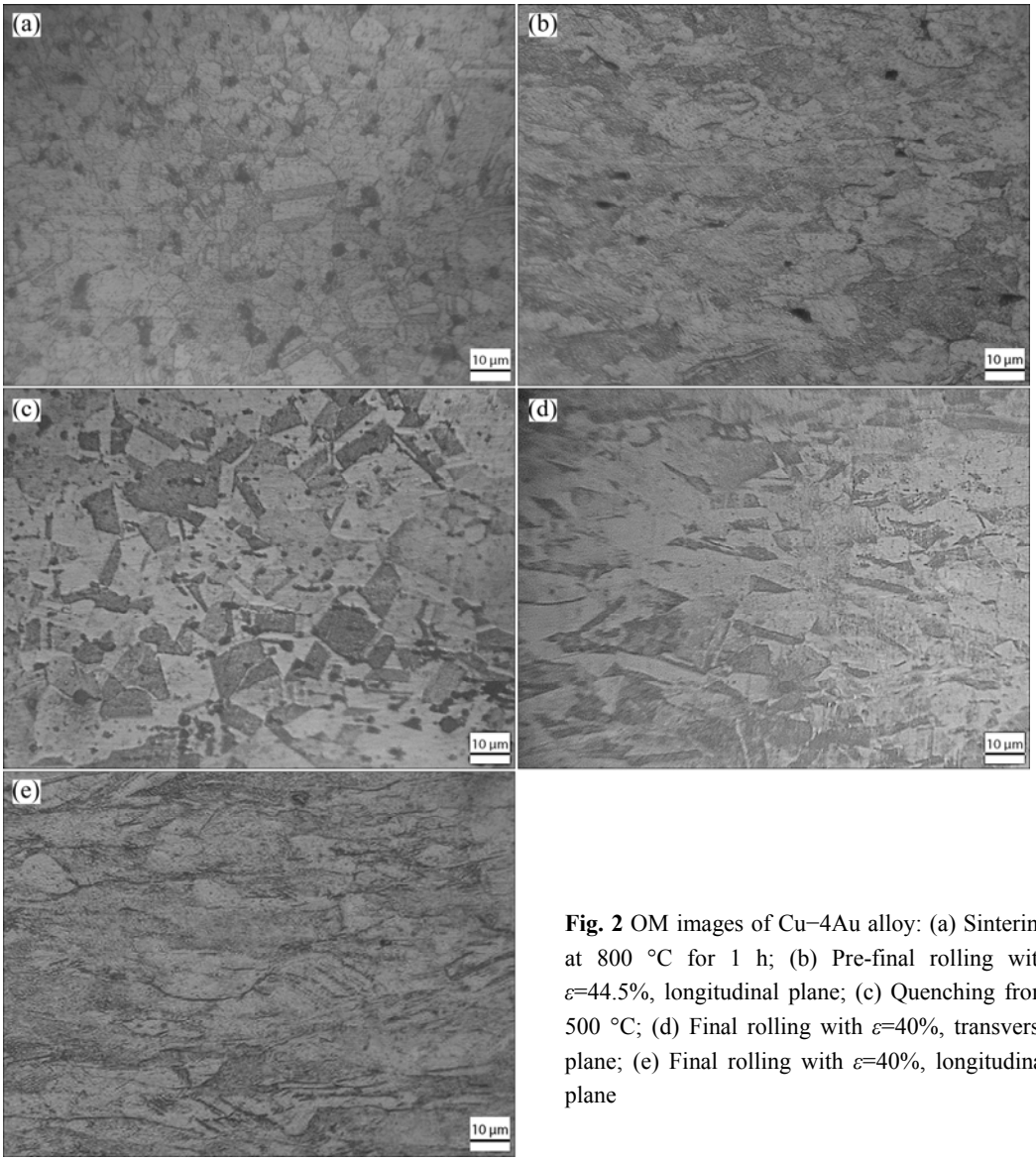

Fig. 2 OM images of Cu−4Au alloy: (a) Sintering at 800 °C for 1 h; (b) Pre-final rolling with ε=44.5%, longitudinal plane; (c) Quenching from 500 °C; (d) Final rolling with ε=40%, transverse plane; (e) Final rolling with ε=40%, longitudinal plane

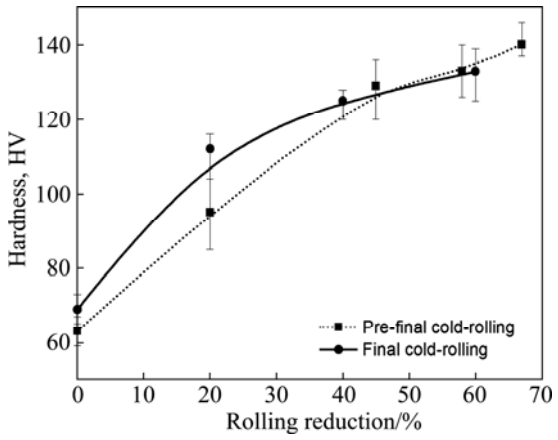

Fig. 3 Influence of rolling reduction on hardness during pre-final and final cold-rolling

hardness value is HV69 and during the final rolling with 60% reduction, it increases to HV133. It can be seen that the quenched sample has a higher hardness value than that of the sintered sample, because of an increase in mechanical properties caused by an increase in the density of samples and an increase in the concentration of point defects in the lattice [21]. A high concentration of thermal vacancies is retained by quenching from high temperatures, causing a greater increase in the hardness of the quenched sample compared to the sintered sample [22].

Figure 4 shows the influence of rolling reduction on the microhardness values during the pre-final and final cold-rolling. As the rolling reduction increases, the microhardness values steadily increase. The microhardness value of the sintered sample is HV102. After the pre-final cold-rolling with 66.7% reduction, this value reaches HV172. The microhardness value of the quenched sample is HV103 and it increases to HV174 after the final rolling with 60 % reduction. The finally rolled samples exhibit higher hardness values than the pre-finally rolled samples, throughout the range of

rolling reductions. During the rolling with lower rolling reductions, the microhardness values of quenched samples increase slightly faster than the microhardness values of sintered samples, because the quenched microstructure has more point defects than the microstructure of the sintered sample. The large amount of point defects and the formation of vacancy clusters in the quenched sample create more difficulties in the movement of dislocations, causing it to harden faster [23].

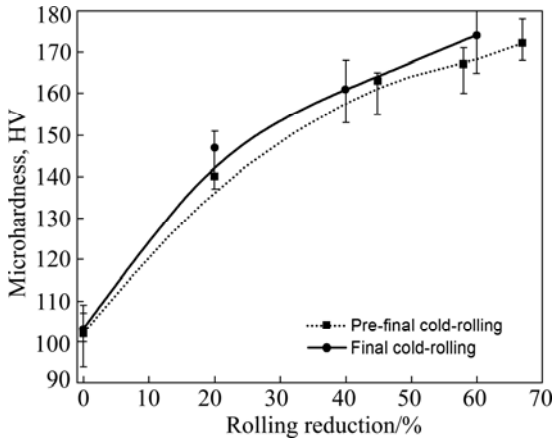

Fig. 4 Influence of rolling reduction on microhardness during pre-final and final cold-rolling

Figure 5 shows the influence of rolling reduction on the electrical conductivity values during the pre-final and final cold-rolling. The electrical conductivity values increase with the increase in rolling reduction up to 40%−50%, and then decrease slowly as the rolling reductions further increase for both pre-finally and finally rolled samples. The electrical conductivity value of the sintered sample increases significantly, from 24.98 to 30.15 MS/m, after pre-final rolling with a 44.5% reduction. Further increase in rolling reduction causes a decrease in electrical conductivity to 29.23 MS/m after pre-final rolling with 66.7% reduction. The electrical conductivity value of the quenched samples is 29.24 MS/m and it increases to 29.8 MS/m after the final rolling with a 40% reduction. After the final rolling with a 60% reduction, the electrical conductivity of the quenched sample decreases to 28.61 MS/m.

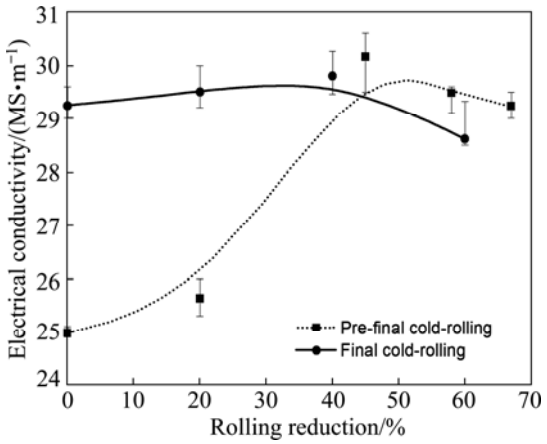

Fig. 5 Influence of rolling reduction on electrical conductivity during pre-final and final cold-rolling

Electrical conductivity is very sensitive to the density of the samples and the concentration of lattice defects. It increases with an increase in density of the samples and with a decrease in the concentration of lattice defects. Sintered samples are porous, but porosity decreases during the rolling due to sealing of the pores [14]. Lattice defects are electron scatterers, and their increase during the rolling causes a decrease in electrical conductivity [23]. During the rolling with low rolling reductions, the effect of the porosity decrease is dominant, causing an increase in electrical conductivity. However, with a further increase in the rolling reduction, increase in the number of dislocations and the lattice distortion become dominant, causing a decrease in electrical conductivity [24,25].

During the rolling with higher rolling reductions than about 45%, the hardness (Fig. 3) and electrical conductivity values (Fig. 5) of the pre-finally rolled samples (with initial sintered microstructure) are higher than the values of the finally rolled samples (with initial microstructure of quenched pre-finally rolled samples). This has occurred due to the more intensive increase in the density of the sintered samples during the pre-final rolling with higher rolling reductions compared to the lower increase in the density of the relatively compacted quenched samples during the final rolling with higher rolling reductions.

3.2 Influence of annealing on properties and microstructure

Figure 6 shows the influence of annealing on the hardness values of quenched and finally rolled samples with 20% and 40% reduction

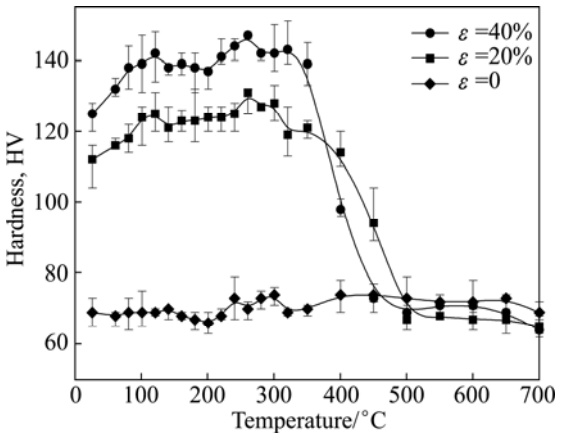

Fig. 6 Influence of annealing on hardness values

When the finally rolled samples are annealed at temperatures in the range of 60 to 350 °C, they strengthen as a result of the anneal hardening effect. An increase in hardness takes place in two stages, corresponding to the primary and secondary hardening. During the annealing at temperatures lower than 200 °C, the primary hardening is noticeable. After transitioning through the peak of this stage, the hardness decreases slightly, and then the secondary hardening stage between 200 and 350 °C occurs. The maximum increase in hardness is achieved during the secondary hardening stage after annealing at 260 °C. The hardness value of the finally rolled sample with 40% reduction is HV125, and during the primary hardening stage it increases to HV142, then it slightly decreases and increases again during the secondary hardening stage when it reaches its maximum of HV147, after annealing at 260 °C. The hardness value of the finally rolled sample with 20% reduction is HV112 and it increases to HV125 after annealing during the primary hardening stage. The hardness maximum of HV131 is achieved during the secondary hardening stage, after annealing at 260 °C. Finally rolled samples with 20% and 40% reduction after annealing at 260 °C achieve an absolute hardness increase of HV19 and HV22, respectively, corresponding to the increase in relative hardness of 17% and 17.6%, respectively. This confirms that the intensity of the anneal hardening effect increases with an increase in the reduction of previous rolling, as some other studies reported [6,7,10,14−16]. The hardness value of the quenched sample in un-deformed state is HV69, and it increases slightly up to HV73, after annealing in the temperature range between 250 and 300 °C. Similar results were obtained by VITEK and WARLIMONT [6] and TOMOKIYO et al [10]. They concluded that the anneal hardening effect could not be observed in the quenched samples because of the lower concentration of defects compared to the deformed samples.

Numerous researches on the mechanism of anneal hardening in various copper-based alloys have been done, but there is no clear indication of the nature of this strengthening mechanism to this day. Based on the measurements of the specific heat, electric specific resistance and dilatometric measurements in Cu−Al alloys, SUGINO et al [26] proposed a concept of partial long-range ordering of the Cu_3Al superlattice in order to explain the origin of this phenomenon. KUWANO et al [27] showed that the anneal hardening effect in concentrated alloys could not be explained only by the segregation of solute atoms due to the Suzuki effect. An increase in the asymmetry of the diffraction line profile and the discovered superlattice reflection indicate a locally ordered structure. They confirmed that anneal hardening was related to the deformation-induced defects and to the short-range ordering. The ordered regions grew mainly at stacking faults, causing a coherent strain around them. However, according to MIURA and TAJIMA [13], solute segregation was responsible for this strengthening mechanism, and grain boundaries played a significant role as well. Dislocations accumulated close to the grain boundaries, causing a large amount of lattice distortion, which in turn caused the diffusion of solute atoms and formation of Suzuki locking atmosphere. VITEK and WARLIMONT [6] also concluded that the segregation of solute atoms to dislocations was the main reason for hardening during the low temperature annealing. They showed that the intensity of anneal hardening in dilute copper alloys depended on the properties of solute atoms, which determined the amplitude and efficiency of their segregation at deformation-induced dislocations.

Figure 7 shows the influence of annealing on the microhardness values of the quenched and finally rolled samples with 20 % and 40 % reduction. It can be seen from Figs. 6 and 7 that the relation between the microhardness and the annealing temperature has nearly the same tendency as the described relation between the hardness and the annealing temperature. Thus, for the finally rolled samples, an increase in microhardness takes place in two stages, similar to the hardness values. The microhardness value of the finally rolled sample with 40% reduction is HV161 and it increases to HV177 after annealing during the primary hardening stage. The maximum microhardness of HV186 is reached after annealing at 260 °C. The microhardness value of the finally rolled sample with 20% reduction is HV147 and it increases to HV162, then it slightly decreases and increases again, reaching its maximum of HV 165 after annealing at 260 °C. This means that the finally rolled samples with 20% and 40% reduction annealed at 260 °C reach the absolute increase in hardness of HV18 and HV27, respectively, i.e., a relative increase in hardness of 12.2% and 16.8%, respectively. The microhardness value of the quenched sample is HV103, and it remains

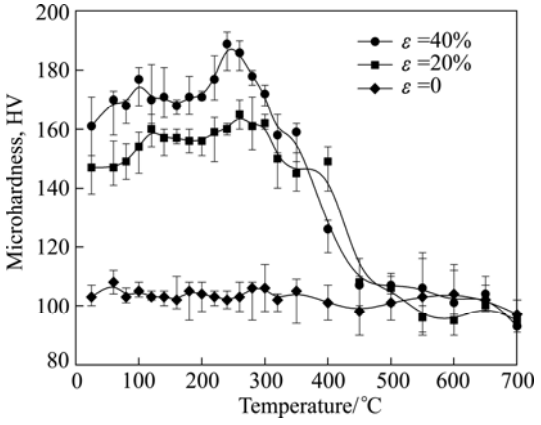

Fig. 7 Influence of annealing on microhardness values

almost unchanged during the annealing, similar to the hardness behaviour of the quenched sample.

Figure 8 shows the influence of annealing on the electrical conductivity values of quenched and finally rolled samples with 20% and 40% reduction.

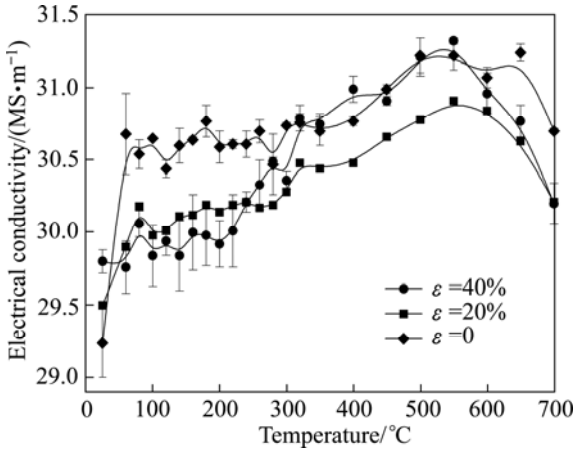

Fig. 8 Influence of annealing on electrical conductivity values

Electrical conductivity is one of the properties most sensitive to the concentration of vacancies because they are potent electron scatterers [23]. It can be seen that the greatest increase in electrical conductivity during the annealing at 60 °C is achieved in the quenched sample. The electrical conductivity of the quenched sample increases from 29.24 to 30.68 MS/m after annealing at 60 °C, and then continues to increase slightly, reaching its maximum of 31.22 MS/m after annealing at 550 °C, before decreasing. The electrical conductivity in the quenched state increases rapidly during the annealing, as a result of thermal removal of vacancies from the material. This is a result of the migration of vacancies to the regions of discontinuity in the structure (e.g. free surfaces, grain boundaries or dislocations) and their annihilation [23].

Increasing the annealing temperature from 25 to 550 °C results in an increase in the electrical conductivity of the finally rolled sample with 20% reduction. The electrical conductivity of the finally rolled sample with 40% reduction increases continually during the low-temperature annealing to 550 °C. In the temperature range between 200 and 300 °C, where the hardness and microhardness values show a significant increase too, a sudden increase in the electrical conductivity of the finally rolled sample with 40% reduction is evident. The electrical conductivity of the finally rolled samples increases with increase of the annealing temperature to 350−400 °C. This increase indicates that the number of dissolved gold atoms in the solid solution decreases, and the segregation of gold atoms at dislocation takes place. Similar results have been reported by BADER et al [7]. Further annealing at a higher temperature causes a recrystallization, a decrease in the density of dislocation and the growth of grains, resulting in a further increase in electrical conductivity [28]. However, it can be seen that the electrical conductivity of all samples decreases above 500−550 °C. RAYGAN et al [29] explained this decrease as a result of some order-disorder transformations which occur in certain copper-based systems such as the Cu−Au system.

Figures 9 and 10 show SEM images and OM images of finally rolled samples with 40% reduction after annealing at 260 and 700 °C, respectively. Figures 9(a), 9(b), 10(a) and 10(b) show the microstructure of finally rolled samples with 40% reduction after annealing at 260 °C for a period of 0.5 h. Annealing at 260 °C of finally rolled samples with 40% reduction causes a significant increase in their mechanical properties and

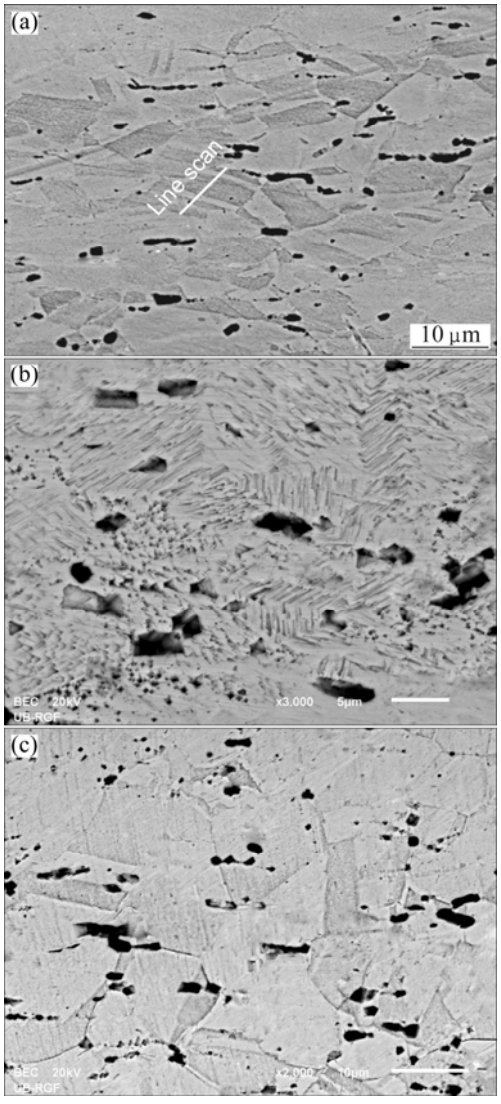

Fig. 9 SEM images of finally rolled alloy with 40% reduction: (a) After annealing at 260 °C for a period of 0.5 h, transverse plane; (b) After annealing at 260 °C for a period of 0.5 h, longitudinal plane; (c) After recrystallization annealing at 700 °C for 0.5 h, transverse plane

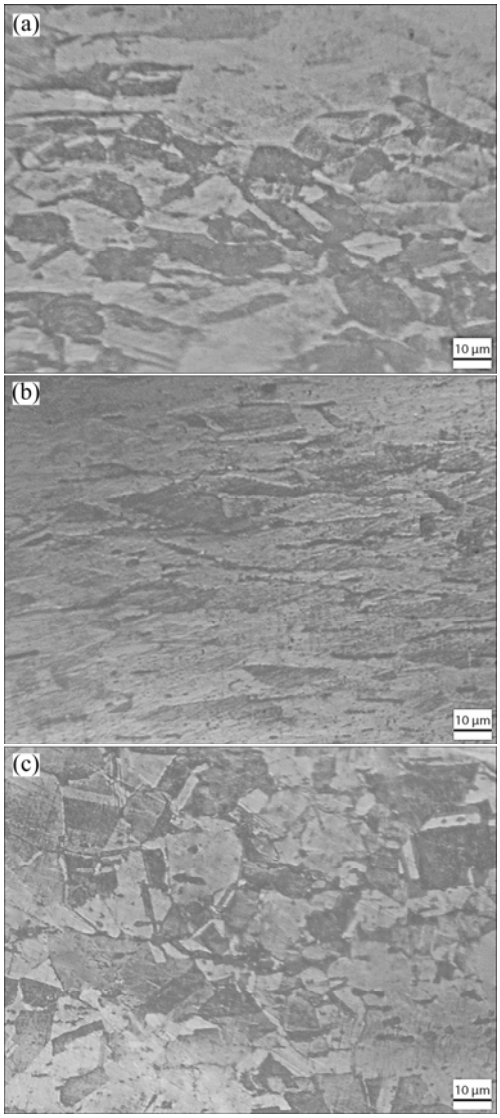

Fig. 10 OM images of finally rolled alloy with 40% reduction: (a) Annealing at 260 °C for a period of 0.5 h, transverse plane; (b) Annealing at 260 °C for a period of 0.5 h, longitudinal plane; (c) Recrystallization annealing at 700 °C for 0.5 h, transverse plane

electrical conductivity, but according to the presented microstructures, there are no significant differences between the annealed and deformed structures. Grains are still elongated in the rolling direction and the deformation structure is still visible. In the longitudinal plane, strain markings are still visible. NISHINO [30] showed that slip lines could not be detected in Cu−Al alloys with less than 3% aluminium (mass fraction). It was concluded that the slip lines were created because of non-uniform distribution of accumulated solute atoms and vacancies, rather than piled-up dislocations. It was shown that during the annealing, the places where slip lines were bent were locally divided into smaller straight line segments. Therefore, slip lines were fragmented. This occurrence became intensified with the prolongation of the annealing time and with an increase in the concentration of the solute atoms. Because of the relatively short annealing time and a low gold content, this tendency was not clearly noticeable in the Cu−Au samples.

The line along which the EDS analysis was performed is shown in Fig. 9(a). Figure 11 shows the variation of gold content within the grain of finally rolled samples with 40% reduction after annealing at 260 °C with distance from the beginning of the line shown in Fig. 9(a). It can be seen that the gold content fluctuates from 3.7% to 6% (mole fraction). This un-homogeneity in gold content confirms the enrichment and impoverishment of certain areas with solute atoms due to the segregation of gold atoms at dislocations and the local ordering of the atoms.

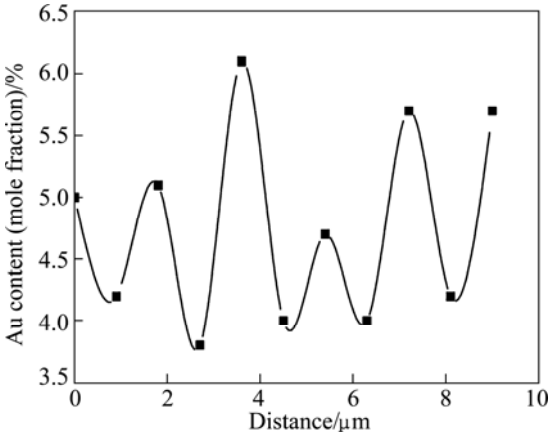

Fig. 11 Variation of gold content along line in Fig. 9(a)

The microstructure of finally rolled sample with 40% reduction after recrystallization annealing at 700 °C is shown in Figs. 9(c) and 10(c). When the annealing temperature reaches 350−400 °C, softening on account of the recrystallization occurs. In the recrystallized microstructure, polygonal and un-deformed twinned grains are clearly noticeable.

4 Conclusions

1) An increase in the rolling reduction during the pre-final and final rolling results in an increase in hardness, microhardness and electrical conductivity values. During the thermomechanical treatment, significant microstructural changes occur, resulting in changes in the investigated properties.

2) An anneal hardening effect occurs when the cold-rolled alloy is annealed at temperatures up to 350 °C. The increase in all properties is achieved through two stages: the primary hardening up to 200 °C and the secondary hardening at temperatures from 200 to 350 °C. The increase in hardness and microhardness peak values

occurs as a result of the increase in the amount of prior cold-rolling reduction. In the quenched sample, some slight hardening at the expense of anneal hardening is detected. The anneal hardening effect in annealed samples is not accompanied by observable changes in the microstructure, compared to the microstructure in the cold-rolled state.

References

[1] LEE W B, YOON E H, JUNG S B. Effects of fine fiber structures on the mechanical and electrical properties of cold rolled Cu−Ag sheet [J]. Journal of Materials Science Letters, 2003, 22(24): 1751−1754.

[2] SONG Ke-xing, XING Jian-dong, TIAN Bao-hong, LIU Ping, DONG Qi-ming. Influence of annealing treatment on properties and microstructures of alumina dispersion strengthened copper alloy [J]. Transactions of Nonferrous Metals Society of China, 2005, 15(1): 139−143.

[3] LEKKA C, BERNSTEIN N, MEHL M, PAPACONSTANTOPOULOS D. Electronic structure of the $Cu_3Au(111)$ surface [J]. Applied Surface Science, 2003, 219: 158−166.

[4] YU Fang-xin, XIE You-qing, NIE Yao-zhuang, LI Xiao-bo, PENG Hong-jian, TAO Hui-jin. Electronic structure of Au−Cu alloys [J]. Transactions of Nonferrous Metals Society of China, 2004, 14(6): 1041−1049.

[5] ROSNER H, KUHLMANN O, NEMBACH E. Dislocation configurations in ordered copper-10 at.% gold solid solutions [J]. Materials Science and Engineering A, 1998, 242: 296−298.

[6] VITEK J M, WARLIMONT H. The mechanism of anneal hardening in dilute copper alloys [J]. Metallurgical Transactions A, 1979, 10: 1889−1892.

[7] BADER M, ELDIS G T, WARLIMONT H. The mechanisms of anneal hardening in Cu−Al alloys [J]. Metallurgical Transactions A, 1976, 7: 249−254.

[8] VARSCHAVSKY A, DONOSO E. DSC Evaluations in f.c.c. solid solutions of short-range-order kinetics as influenced by bound vacancies [J]. Journal of Thermal Analysis and Calorimetry, 2000, 63(2): 397−413.

[9] VARSCHAVSKY A, DONOSO E. Short-range-ordering kinetics of Cu−5at% Zn influenced by solute-vacancy complexes and cold rolling [J]. Journal of Thermal Analysis and Calorimetry, 2001, 65(1): 185−195.

[10] TOMOKIYO Y, KUWANO N, EGUCHI T. Short range ordering in deformed αCu−Al alloys [J]. Transactions of the Japan Institute of Metals, 1975, 16: 489−499.

[11] VARSCHAVSKY A, DONOSO E. A calorimetric investigation on the kinetics of solute segregation to partial dislocations in Cu−3.34at%Sn [J]. Materials Science and Engineering A, 1998, 251(1−2): 208−215.

[12] VARSCHAVSKY A, DONOSO E. Modelling the kinetics of solute segregation to partial dislocations in cold-rolled copper alloys [J]. Materials Letters, 1997, 31(3): 239−245.

[13] MIURA S, TAJIMA T. Effect of grain boundaries on anneal hardening in Cu−Al alloy [J]. Metal Science, 1978, 12(4): 183−191.

[14] NESTOROVIC S, RANGELOV I, MARKOVIC D. Improvements in properties of sintered and cast Cu−Ag alloys by anneal hardening effect [J]. Powder Metallurgy, 2011, 54(1): 36−39.

[15] NESTOROVIC S. Influence of alloying and secondary annealing on anneal hardening effect at sintered copper alloys [J]. Bulletin of Materials Science, 2005, 28(5): 401−403.

[16] NESTOROVIC S, MARKOVIC D. Influence of alloying on the anneal hardening effect in sintered copper alloys [J]. Materials transactions JIM, 1999, 40(3): 222−224.

[17] NAGARJUNA S, BALASUBRAMANIAN K, SARMA D S. Effect of prior cold work on mechanical properties, electrical conductivity and microstructure of aged Cu−Ti alloys [J]. Journal of Materials Science, 1999, 34(12): 2929−2942.

[18] COUPEAU C, BONNEVILLE J, MATTERSTOCK B, GRILHÉ J, MARTIN J L. Slip line analysis in Ni_3Al by atomic force microscopy [J]. Scripta Materialia, 1999, 41(9): 945−950.

[19] KUBIN L P, ESTRIN Y. Strain nonuniformities and plastic instabilities [J]. Revue de Physique Appliquée (Paris), 1988, 23: 573−583.

[20] FREUDENBERGER J. Copper alloys preparation, properties and applications, Chapter 9. High strength copper-based conductor materials [M]. New York: Nova Science Publishers Inc, 2011.

[21] WU Di, TANG Wei-neng, CHEN Rong-shi, HAN En-hou. Strength enhancement of Mg−3Gd−1Zn alloy by cold rolling [J]. Transactions of Nonferrous Metals Society of China, 2013, 23: 301−306.

[22] YOSHIMI K, HANADA S, YOO M H. On lattice defects and strength anomaly of B2-type FeAl [J]. Intermetallics, 1996, 4: S159−S169.

[23] SHALLMAN R E, BISHOP R J. Modern physical metallurgy and materials engineering [M]. London: Butterworth-Heinemann, 1999.

[24] CHANDLER H. Heat treater's guide: practices and procedures for nonferrous alloys [M]. Ohio: ASM International, 1996.

[25] ÇETINARSLAN C. Effect of cold plastic deformation on electrical conductivity of various materials [J]. Materials and Design, 2009, 30: 671−673.

[26] SUGINO S, NAKANISHI N, MITANI H. Anomalous phenomena in α phase Cu−Al binary alloys [J]. Bulletin of University of Osaka Prefecture. Series A: Engineering and Natural Sciences, 1964, 12(2): 97−107.

[27] KUWANO N, TOMOKIYO Y, KINOSHITA C, EGUCHI T. Study of annealing effects on cold-worked α phase of Cu−Al alloys [J]. Transactions of the Japan Institute of Metals, 1974, 15: 338−344.

[28] ZHU Da-chuan, TANG Ke, SONG Ming-zhao, TU Ming-jing. Effect of annealing process on electrical conductivity and mechanical property of Cu−Te alloys [J]. Transactions of Nonferrous Metals Society of China, 2006, 16: 459−462.

[29] RAYGAN S, MOFRAD H E, POURABDOLI M, AHADI F K. Effect of rolling and annealing processes on the hardness and electrical conductivity values of Cu−13.5%Mn−4%Ni alloy [J]. Journal of Materials Processing Technology, 2011, 211(11): 1810−1816.

[30] NISHINO K. Study of anneal hardening of copper alloys [J]. Bulletin of the Yamagata University, 1959, 5(2): 410−436.

形变热处理对烧结 Cu−Au 合金性能与微观组织的影响

Ivana MARKOVIC, Svetlana NESTOROVIC, Desimir MARKOVIC, Dragoslav GUSKOVIC

Technical faculty in Bor, University of Belgrade, VJ 12, 19210 Bor, Serbia

摘　要：研究 Cu−4%Au 合金的硬度、显微硬度、导电性和微观组织在形变热处理过程中的变化。在加工硬化后，再对轧制合金在 60~350 °C 温度下退火。由于退火硬化效应，合金的强度增大。结果表明：Cu−Au 合金性能在两个阶段都得到改善；合金进行变形量为 40%的热轧后，在 260 °C 退火能得到最佳的综合性能。合金的微观组织也在形变热处理过程中发生显著变化。

关键词：Cu−Au 合金；退火硬化；形变热处理；硬度；显微硬度；电导率

(Edited by Chao WANG)